Chinese Journal of Aeronautics

Optimizing Interplanetary Trajectories Bezier Shape-Based Method Applied to Magnetic Sail

--Manuscript Draft--

Manuscript Number:	CJOA-D-25-01577
Article Type:	VSI: 2025 AFC-Original Article
Section/Category:	Flight Vehicle Design
Keywords:	magnetic sail; thrust model; Bezier shape-based method; rapid trajectory optimization; preliminary mission analysis; inter-planetary spaceflight
Corresponding Author:	Mingying Huo Harbin Institute of Technology CHINA
First Author:	Borui Yao
Order of Authors:	Borui Yao
	Ruhao Jin
	Hanqing Zhao
	Ziqi Hao
	Lehan Wang
	Junhao Jiang
	Yuhao Shi
	Yihang Fu
	Jiaqi Yue
	Mingying Huo
Abstract:	Interplanetary spaceflight is vital for deep space exploration, yet severely hampered by fuel constraints. Magnetic sails, a fuel-free propulsion system with a high thrust-to-weight ratio, have become a research hotspot. This study improves the Single-Loop Magnetic Sail (SiLM) thrust model via precise coil current control, enhancing its adaptability to complex deep-space missions. To optimize magnetic sail interplanetary trajectories rapidly, a Bezier curve parameterization strategy is proposed. By assuming magnetic sail state parameters follow Bezier curves, coefficients are optimized for time efficiency under motion and constraint equations. In the Earth-to-Mars transfer mission validation, the trajectory accuracy difference between the Bezier method and the GPM was less than 2%, while the computational speed of Bezier method increased by approximately 23 times, underscoring its advantages in rapid analysis for multiple scenarios during the early mission phases. Research on magnetic sail design parameters reveals a nonlinear link between coil radius and shortest flight time, guiding performance parameter design. The Bezier method also excels in solar system escape mission validation, proving its universality. This study developed an improved magnetic sail thrust model and a rapid trajectory optimization method, providing an efficient theoretical tool for orbit design and system parameter optimization in deep space exploration missions.

Optimizing Interplanetary Trajectories Bezier Shape-Based Method Applied to Magnetic Sail

Abstract

Interplanetary spaceflight is one of the indispensable means for deep space exploration, yet it is highly constrained by the limitations imposed by fuel loading. As a propulsion system that operates without fuel, magnetic sails have garnered increasing attention and research focus due to their high thrust-to-weight ratio. This study adopts the latest Single-Loop Magnetic Sail(SiLM) thrust model and employs precise control of the coil current to construct an improved magnetic sail thrust model, thereby enhancing its suitability for complex deep-space exploration missions. To achieve rapid trajectory optimization for magnetic sail interplanetary missions, this study proposes an optimization strategy based on Bezier curve parameterization. Assuming that the variation of the magnetic sail state parameters follows a Bezier curve form, the Bezier coefficients are optimized under a time-optimal objective to satisfy the equations of motion and constraint conditions. In this study, a typical deep space exploration scenario is designed for simulation validation. The results obtained using the Bezier method serve as the initial guess for the Gauss Pseudo-spectral Method(GPM), which is subsequently further optimized to compare the performance of the two methods. In the Earth-to-Mars transfer mission validation, the trajectory accuracy difference between the Bezier method and the GPM was less than 2%, while the computational speed of Bezier method increased by approximately 23 times, underscoring its advantages in rapid analysis for multiple scenarios during the early mission phases. Furthermore, the influence of magnetic sail design parameters on the transfer trajectory was investigated. By altering the magnetic sail coil radius, a nonlinear relationship curve between the shortest flight time and the coil radius was obtained, providing significant guidance for the design of magnetic sail performance parameters. In the validation of the solar system escape mission, the Bezier method still maintained excellent performance advantages, demonstrating its universality. This study developed an improved magnetic sail thrust model and a rapid trajectory optimization method, providing an efficient theoretical tool for orbit design and system parameter optimization in deep space exploration missions.

Keywords: magnetic sail; thrust model; Bezier shape-based method; rapid trajectory optimization; preliminary mission analysis; interplanetary spaceflight

1. Introduction

Deep space exploration is one of the key methods for humanity to investigate the universe, holding significant importance for scientific research and future development. In recent years, deep space exploration has entered a new phase of activity.

Interplanetary navigation is an essential means for deep space exploration. Chemical fuel propulsion has drawbacks such as limited propellant carrying capacity, the necessity for gravity-assisted maneuvers and limited launch

opportunities. New propellant - less continuous - thrust propulsion technologies that utilize external resources like solar energy and solar wind have emerged as effective solutions. These propulsion methods use solar light and solar wind plasma as working media[1], including solar sails[2-5], electric sails[6-8], magnetic sails[9-12], etc. Magnetic sails possess excellent characteristics and show great potential in deep space exploration propulsion methods. In this study, the single - loop magnetic sail thrust model (SiLM) proposed by Mengali et al. is adopted and improved.

In recent years, numerous scholars have achieved results in the field of spacecraft trajectory research. Petropoulos et al.[13] proposed the shape method, using exponential sine functions to describe the spacecraft's flight trajectory and optimizing relevant coefficients to meet the corresponding constraint conditions. Wall, Conway et al.[14] utilized inverse polynomials to solve the radial distance of the planar trajectory in the polar coordinate system. Xie et al.[15] presented an approximation method for low - thrust trajectories considering the trajectory constraints between two coplanar elliptical orbits. Peloni et al.[16] approximated the transfer trajectory in the spacecraft rendezvous mission by combining exponential terms and sine terms. Taheri and Abdelkhalik[17] adopted the Finite Fast Fourier Series (FFS) shape method. Under the consideration of thrust vector constraints, they obtained the two - dimensional and three - dimensional transfer trajectories of low - thrust spacecraft. This method expands the time - variation of the spacecraft's state through the Fourier series and determines the coefficients based on the optimization of performance indicators and boundary constraints. Huo et al.[18] designed the transfer trajectory of an electric sail for asteroid exploration using Bezier curves. They assumed that the time - variation of spacecraft state variables conforms to the form of a Bezier curve function. Some coefficients were analytically calculated through boundary constraints, and the remaining unknown coefficients were calculated by minimizing total flight time while taking into account the constraints on the magnitude and direction of the electric sail thrust vector.

This paper is structured in the following manner. Chapter 2: establishing the mathematical model for magnetic sail trajectory optimization. Chapter 3: trajectory optimization of magnetic sails using Bezier functions. Chapter 4: simulation verification and analysis. Chapter 5: conclusions of research findings.

2. Mathematical Model of the Trajectory Optimization Problem

2.1. Definition of Coordinate System

In order to facilitate the description of the heliocentric transfer path of the magnetic sail spacecraft, this study employs the heliocentric ecliptic coordinate system $(o_i x_i y_i z_i)$.(ρ,θ,z), the spacecraft orbital coordinate system , the cylindrical coordinate system , and the spacecraft body coordinate system, as illustrated in Fig.1. $(o_i x_i y_i z_i)$ has its origin o_i at the Sun, x_i -axis points to the vernal equinox at J2000, z_i -axis is perpendicular to the ecliptic plane, the y_i -axis, x_i -axis and z_i -axis form a right-handed coordinate system. $(o_o x_o y_o z_o)$ has its origin o_o at the spacecraft, z_o -axis points the vector direction from the Sun to the spacecraft. The y_o -axis is perpendicular to the z_o -axis and is also perpendicular to the z_i -axis. It also satisfies the requirements of a right-handed coordinate system. (ρ,θ,z) also has its origin at sun, ρ is the projection of the vector from the Sun to the spacecraft position onto the $x_i o_i y_i$ plane. θ is the angle between vector ρ and the x_i -axis, z is the altitude of the spacecraft above the ecliptic plane. In order to facilitate the description of the thrust generated by the magnetic sail, we establish a body-fixed coordinate system of the magnetic sail $(o_b x_b y_b z_b)$. It has its origin at the center of mass of the magnetic sail, z_b -axis points towards the direction of the magnetic dipole moment (MDM) vector, the y_b -axis is perpendicular to the plane formed by the z_b -axis and the z_o -axis. It also satisfies the requirements of a right-handed coordinate system

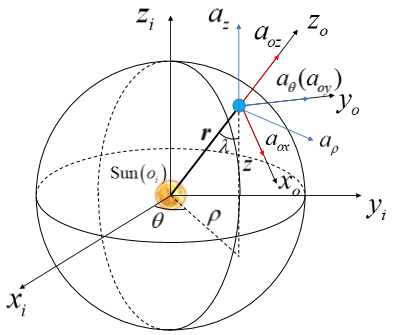

(a) Heliocentric ecliptic coordinate system, spacecraft orbital coordinate system, and cylindrical coordinate system

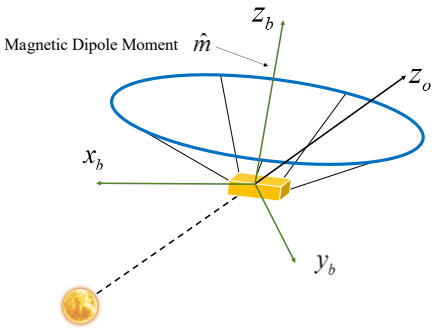

(b) Body-fixed coordinate system of the magnetic sail

Fig.1 Various coordinate systems for the motion of magnetic sails within the solar system

2.2. Magnetic Sail Propulsion Acceleration Model

Based on the latest single-loop magnetic sail(SiLM) thrust model proposed by Mengali et al.[12], this study rigorously controls the coil current to improve the magnetic sail thrust model, enabling it to be better suited for complex planetary exploration missions and facilitating subsequent trajectory optimization. The derivation process is as follows.

SiLM thrust model is presented as follows:

$$\vec{F} = \vec{F}^{ref}\left(\frac{r^{ref}}{r}\right)^2\left(\frac{R}{R^{ref}}\right)^2\left[\frac{\ln\left(\dfrac{cI}{v_{SW}I_c}\right)}{\ln\left(\dfrac{cI^{ref}}{v_{SW}^{ref}I_c}\right)}\right]^n \tag{1}$$

where r represents the distance between the magnetic sail and the Sun, R is the radius of the magnetic sail's coil, I denotes the current in the coil, v_{SW} is the solar wind speed, I_c is the critical current, and n is a constant. The superscript '*ref*' indicates the parameters corresponding to the reference magnetic sail.

Since the acceleration of the magnetic sail is determined by the thrust vector divided by the total mass of the sail, we first investigate the optimal mass of the magnetic sail. The relationship between the SiLM's mass and the coil's mass m_{coil} is outlined in the equation below:

$$m_{sail} = 3.75m_{coil} \tag{2}$$

According to the research by Zubin and Andrews[9, 19], m_{coil} depends on the R, the I, the mass density of the coil ρ, and the current density J. The specific expressions are as follows:

$$m_{coil} = 2\pi R\rho\frac{I}{J} \tag{3}$$

By combining Eqs. (2) and (3), the total mass of the magnetic sail can be obtained:

$$m_{tot} = m_{pay} + 3.75m_{coil} = m_{pay} + kRI \tag{4}$$

where m_{pay} represents the payload mass $m_{pay} = fm_{tot}$, $f \in (0,1)$ is the dimensionless coefficient, $k \triangleq 7.5\pi\rho / J \approx 1.49\times10^{-5}\,\mathrm{kg/m}$, and m_{tot} can be rewritten as follows:

$$m_{tot} = \frac{kRI}{1-f} \tag{5}$$

It is straightforward to derive the relationship between the magnitude of the magnetic sail's propulsion acceleration a and $\{r, R, I, v_{SW}\}$, as expressed in the following equation:

$$a \propto \frac{R\left[\ln\left(\dfrac{cI}{v_{SW}I_c}\right)\right]^n(1-f)}{r^2I} \tag{6}$$

By maximizing $\left[\ln\left((cI)/(v_{SW}I_c)\right)\right]^n / I$, the maximum propulsion acceleration of the magnetic sail can be achieved. The specific value of I is as follows:

$$I = I_0 \triangleq \frac{e^n v_{SW}I_c}{c} \tag{7}$$

Substituting I_c into Eq. (5), we obtain the optimal mass of the magnetic sail $m_{tot} = kRI_0 / (1-f)$. Combining this with Eq. (1), we derive the expression for the acceleration of the magnetic sail:

$$\vec{a} = \frac{(1-f)}{kRI_0}\left(\frac{r^{ref}}{r}\right)^2\left(\frac{R}{R_{ref}}\right)^2\left[\frac{\ln\left(\frac{cI}{v_{SW}I_c}\right)}{\ln\left(\frac{cI^{ref}}{v_{SW}^{ref}I_c}\right)}\right]^n \vec{F}^{ref} \tag{8}$$

This model neglects fluctuations in the solar wind and takes into account the component of the magnetic sail's velocity in the direction of the solar-magnetic sail vector $|v\cdot\hat{r}| \ll v_{SW}$, reasonable assumed $v_{SW} \simeq v_{SW}^{ref}$.

By controlling *I* in the Eq. (8), we derive an improved acceleration model for the magnetic sail. To simplify the mathematical form of the acceleration model as much as possible, this study sets *I* to satisfy the following form:

$$I = e^{n\left(\gamma^{1/n}-1\right)}I_0 = \frac{e^{n\cdot\gamma^{1/n}}\cdot v_{SW}I_c}{c} \tag{9}$$

Integrating Eq. (9) with Eq. (8) established an improved propulsion model for magnetic sails:

$$\vec{a} = \frac{\gamma KR(1-f)}{r^2}\vec{F}^{ref} \tag{10}$$

where $K \simeq 1.735\times10^{-5}\,\mathrm{kg^{-1}\cdot m^{-1}}$ is a constant, and $\gamma \in [0,1]$ is the thrust coefficient. When $\gamma = 0$, it indicates that the magnetic sail is in the gliding phase during the transfer process. It is noteworthy that under this thrust acceleration model, the magnetic sail's primary design variables are reduced to *R* and *f*. This simplification facilitates the early design of deep space exploration missions, allowing for mission planning to be conducted by solely adjusting *R* and *f*.

Based on the thrust model for magnetic sails introduced by Quarta et al.[10], it can be categorized into two modes of magnetopause: 'thin' and 'thick'. The acceleration of the magnetic sail can be expressed as:

$$\vec{a} = a_c\tau\left(\frac{r_\oplus}{r}\right)^\eta\left(C_D\hat{i}_r + C_L\hat{i}_v\right) \tag{11}$$

where

$$\begin{aligned} C_D &= h_0 + h_1\cos(2\beta) \\ C_L &= k_0\sin(2\beta) + k_1\sin(4\beta) \end{aligned} \tag{12}$$

r is the distance between the Sun and the magnetic sail, while β is the solar incidence angle (the angle between the direction of the solar wind $\hat{i}_r$ and the direction of the magnetic sail's magnetic dipole moment $\hat{m}$). The angle α between the thrust acceleration vector $\hat{a}$ and $\hat{i}_r$ is defined as the thrust cone angle, as shown in Fig.2. a_c represents the characteristic acceleration of the magnetic sail, where C_D and C_L can be parametrized by the solar β that describe the radial and lateral components of the magnetic sail's thrust acceleration vector, respectively.

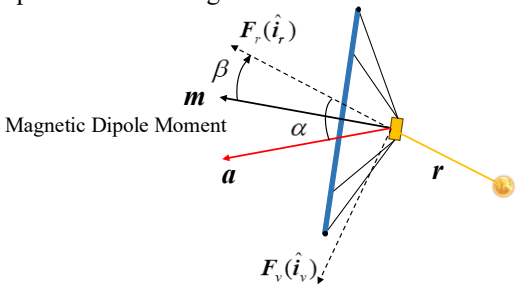

Fig.2 Components of magnetic sail thrust, solar incidence angle, and thrust cone angle

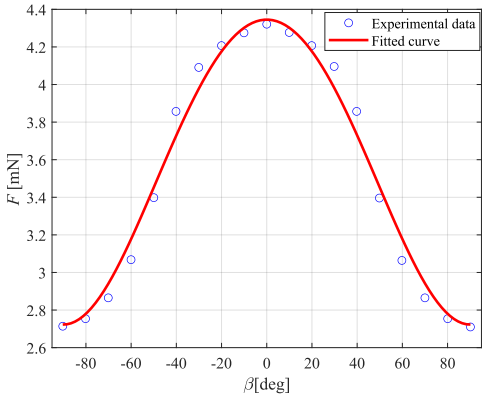

Fig.3 Fitting of magnetic sail thrust curve

Table 1 Optimal fitting coefficients under two different modes[20]

magnetopause mode	h_0	h_1	k_0	k_0	η
thin	0.8133	0.1867	0.1485	0	2
thick	0.8312	-0.1688	-0.1338	0.03969	4/3

This study posits that $\vec{F}^{ref}$ satisfies the component form of the thin mode and introduces a proportional coefficient H, the magnitude of which is determined through data fitting using experimental data provided by Mengali et al., as shown in Figure 3. Therefore, $\vec{F}^{ref}$ is rewritten as:

$$\vec{F}_{ref} = H\left(C_D\hat{i}_r + C_L\hat{i}_v\right) \tag{13}$$

$$\begin{aligned} F_r &= H\left(h_0 + h_1\cos\left(2\beta\right)\right) \\ F_v &= H\left(k_0\sin\left(2\beta\right) + k_1\sin\left(4\beta\right)\right) \end{aligned} \tag{14}$$

where the values of the coefficients are provided in Table 1. By substituting Eq.(14) into Eq.(10), we obtain the complete expression for the improved magnetic sail acceleration model:

$$\vec{a} = \frac{\gamma KR\left(1-f\right)H}{r^2}\left(\left(h_0 + h_1\cos\left(2\beta\right)\right)\cdot\hat{i}_r + k_0\sin\left(2\beta\right)\cdot\hat{i}_v\right) \tag{15}$$

2.3. Magnetic Sail Motion Equation

In this study, the position, velocity, and the propulsion of the magnetic sail are mathematically formulated in a cylindrical polar coordinate framework. It is assumed that during the transfer process, the magnetic sail is only influenced by the gravitational pull of the Sun and its own thrust. The equations of motion for the magnetic sail are as follows:

$$\begin{cases} \ddot{\rho} - \rho\dot{\theta}^2 + \dfrac{\mu_\odot\rho}{r^3} = a_\rho \\ \rho\ddot{\theta} + 2\rho\dot{\theta} = a_\theta \\ \ddot{z} + \dfrac{\mu_\odot z}{r^3} = a_z \end{cases} \tag{16}$$

where μ is the gravitational constant of the central body (the Sun). We further introduce the magnetic sail's thrust clock angle ϕ to describe the thrust acceleration vector, as shown in the Fig.4.

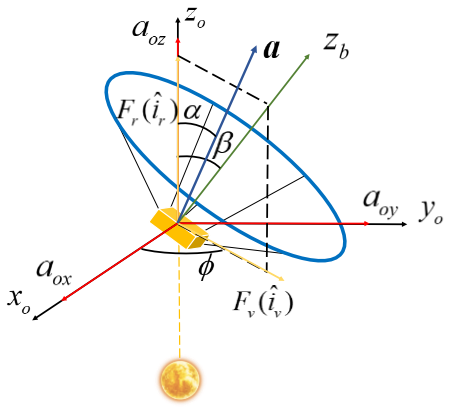

Fig.4 Magnetic sail thrust acceleration

The components of the magnetic sail's acceleration are decomposed into the orbital coordinate system, resulting in the following:

$$\begin{bmatrix} a_{ox} \\ a_{oy} \\ a_{oz} \end{bmatrix} = \frac{\gamma KR(1-f)H}{r^2} \begin{bmatrix} k_0 \sin 2\beta \cos\phi \\ k_0 \sin 2\beta \sin\phi \\ h_0 + h_1 \cos 2\beta \end{bmatrix} \tag{17}$$

Based on the kinematic correspondence between the orbital coordinate system and the cylindrical coordinate system, the components of the magnetic sail thrust acceleration in the cylindrical coordinate system can be expressed as follows:

$$\begin{bmatrix} a_\rho \\ a_\theta \\ a_z \end{bmatrix} = \begin{bmatrix} \cos\lambda & 0 & \sin\lambda \\ 0 & 1 & 0 \\ -\sin\lambda & 0 & \cos\lambda \end{bmatrix} \begin{bmatrix} a_{ox} \\ a_{oy} \\ a_{oz} \end{bmatrix} = \begin{bmatrix} a_{ox}\cos\lambda + a_{oz}\sin\lambda \\ a_{oy} \\ -a_{ox}\sin\lambda + a_{oz}\cos\lambda \end{bmatrix} \tag{18}$$

where $\sin\lambda = \rho / \sqrt{\rho^2 + z^2}$, $\cos\lambda = z / \sqrt{\rho^2 + z^2}$.

2.4. Magnetic Sail Constraints

The magnetic sail conducts a transfer between the initial planet and the target planet. If the transfer time of the spacecraft is known, the spacecraft must satisfy the following boundary constraints on position and velocity:

$$\begin{aligned} &\rho(\tau=0) = \rho_i, \rho'(\tau=0) = T\dot{\rho}_i, \rho(\tau=1) = \rho_f, \rho'(\tau=1) = T\dot{\rho}_f \\ &\theta(\tau=0) = \theta_i, \theta'(\tau=0) = T\dot{\theta}_i, \theta(\tau=1) = \theta_f, \theta'(\tau=1) = T\dot{\theta}_f \\ &z(\tau=0) = z_i, z'(\tau=0) = T\dot{z}_i, z(\tau=1) = z_f, z'(\tau=1) = T\dot{z}_f \end{aligned} \tag{19}$$

where the subscript *'i'* denotes the launch-phase state of the magnetic sail at the initial celestial body, while the subscript *'f'* indicates the arrival parameters of the magnetic sail at the destination celestial body. $\tau = t/T \in [0,1]$ represents the normalized time (dimensionless time), t denotes the current time, and T is the total time of the spacecraft during the transfer process. The symbol '$\cdot$' signifies the derivative with respect to the current time τ, and the superscript ' ' ' denotes the derivative with respect to the normalized time.

In the context of the rendezvous problem involving magnetic sails and target celestial bodies, the boundary conditions for the magnetic sail are constrained by the positional and velocity information at the time of the intersection with the target body. Additionally, when discussing the issue of a magnetic sail escaping the solar system, this problem, from a mathematical perspective, corresponds to specifying the mechanical energy of the magnetic sail at the moment it meets the escape conditions as follows:

$$\varepsilon_f \triangleq -\frac{\mu}{r_f} + \frac{v_f^2}{2} = \frac{v_\infty^2}{2} \tag{20}$$

Where r_f represents the distance from the magnetic sail to the Sun when the escape conditions are met, v_f denotes the flight velocity of the magnetic sail, and v_∞ signifies the transition velocity of the magnetic sail's hyperbolic trajectory. When $v_\infty = 0$, it can be inferred that the magnetic sail has successfully escaped the solar system.

Based on Eq. (17), by eliminating β and ϕ, setting $M=\gamma KR(1-f)H/r^2$, we can derive the following quadratic equation in terms of *M*:

$$\frac{h_0^2-h_1^2}{h_1^2}k_0^2M^2-2\frac{k_0^2a_{oz}h_0}{h_1^2}M+a_{ox}^2+a_{oy}^2+\frac{k_0^2}{h_1^2}a_{oz}^2=0 \tag{21}$$

When $\beta=0\left(a_{ox}=a_{oy}=0\right)$, $M=a_{oz}/\left(h_0+h_1\right)$, a unique solution can be obtained:

$$\gamma=\frac{r^2}{KR(1-f)H}\cdot\frac{a_{oz}h_0k_0^2-h_1^2\sqrt{\frac{k_0^2\left[a_{ox}^2\left(-h_0^2+h_1^2\right)+a_{oy}^2\left(-h_0^2+h_1^2\right)+a_z^2k_0^2\right]}{h_1^2}}}{\left(h_0^2-h_1^2\right)k_0^2} \tag{22}$$

Since $\gamma\in[0,1]$, the following constraint conditions for the magnetic sail acceleration can be obtained:

$$\begin{cases} a_{oz}>0 \\ D=k_0^2\left[a_{ox}^2\left(-h_0^2+h_1^2\right)+a_{oy}^2\left(-h_0^2+h_1^2\right)+a_z^2k_0^2\right]>0 \\ \dfrac{a_{oz}h_0k_0^2-h_1^2\sqrt{\dfrac{k_0^2\left[a_{ox}^2\left(-h_0^2+h_1^2\right)+a_{oy}^2\left(-h_0^2+h_1^2\right)+a_z^2k_0^2\right]}{h_1^2}}}{\left(h_0^2-h_1^2\right)k_0^2}>0 \\ \dfrac{r^2}{KR(1-f)H}\cdot\dfrac{a_{oz}h_0k_0^2-h_1^2\sqrt{\dfrac{k_0^2\left[a_{ox}^2\left(-h_0^2+h_1^2\right)+a_{oy}^2\left(-h_0^2+h_1^2\right)+a_z^2k_0^2\right]}{h_1^2}}}{\left(h_0^2-h_1^2\right)k_0^2}<1 \end{cases} \tag{23}$$

3. Trajectory Optimization Based on Bezier

3.1 State Variable Estimation

In the cylindrical coordinate system of the solar system, the three coordinate components of the magnetic sail are approximately expanded using Bezier functions:

$$\begin{cases} \rho(\tau)=\sum_{j=0}^{n_\rho}B_{\rho,j}(\tau)P_{\rho,j} \\ \theta(\tau)=\sum_{j=0}^{n_\theta}B_{\theta,j}(\tau)P_{\theta,j} \\ z(\tau)=\sum_{j=0}^{n_z}B_{z,j}(\tau)P_{z,j} \end{cases} \tag{24}$$

where n_ρ, n_θ, n_z are the orders of the Bezier functions for the three coordinates, $P_{\rho,j}$, $P_{\theta,j}$, $P_{z,j}$ are the unknown Bezier coefficients, $B_{\rho,j}(\tau)$, $B_{\theta,j}(\tau)$, $B_{z,j}(\tau)$ are the Bezier basis functions, whose specific forms are as follows:

$$\begin{cases} B_{\rho,j}(\tau)=\dfrac{n_\rho!}{j!(n_\rho-j)!}\tau^j(1-\tau)^{n_\rho-j}, \quad j\in[0,n_\rho] \\ B_{\theta,j}(\tau)=\dfrac{n_\theta!}{j!(n_\theta-j)!}\tau^j(1-\tau)^{n_\theta-j}, \quad j\in[0,n_\theta] \\ B_{z,j}(\tau)=\dfrac{n_z!}{j!(n_z-j)!}\tau^j(1-\tau)^{n_z-j}, \quad j\in[0,n_z] \end{cases} \tag{25}$$

Based on Eq. (24), the following derives the first and second derivatives of the three coordinate components with respect to τ:

$$\begin{cases} \rho'(\tau)=\sum_{j=0}^{n_\rho} B'_{\rho,j}(\tau)P_{\rho,j} \\ \theta'(\tau)=\sum_{j=0}^{n_\theta} B'_{\theta,j}(\tau)P_{\theta,j} \\ z'(\tau)=\sum_{j=0}^{n_z} B'_{z,j}(\tau)P_{z,j} \end{cases} \quad \begin{cases} \rho''(\tau)=\sum_{j=0}^{n_\rho} B''_{\rho,j}(\tau)P_{\rho,j} \\ \theta''(\tau)=\sum_{j=0}^{n_\theta} B''_{\theta,j}(\tau)P_{\theta,j} \\ z''(\tau)=\sum_{j=0}^{n_z} B''_{z,j}(\tau)P_{z,j} \end{cases} \tag{26}$$

where $B'_{\rho,j}(\tau)$, $B'_{\theta,j}(\tau)$, $B'_{z,j}(\tau)$, $B''_{\rho,j}(\tau)$, $B''_{\theta,j}(\tau)$, $B''_{z,j}(\tau)$ represent the parametric velocity and acceleration factors in Bezier function space with respect to τ. To avoid redundancy, we will only present the processing procedure for ρ here (the cases of θ and z can be treated similarly):

$$\begin{cases} B'_{\rho,j}(\tau)=\begin{cases} -n_\rho(1-\tau)^{n_\rho-1} & , \quad j=0 \\ \dfrac{n_\rho!\tau^{j-1}(1-\tau)^{n_\rho-j}}{(j-1)!(n_\rho-j)!}-\dfrac{n_\rho!\tau^{j}(1-\tau)^{n_\rho-j-1}}{j!(n_\rho-j-1)!} & , \quad j\in[1,n_\rho-1] \\ n_\rho\tau^{n_\rho-1} & , \quad j=n_\rho \end{cases} \\ B''_{\rho,j}(\tau)=\begin{cases} n_\rho(n_\rho-1)(1-\tau)^{n_\rho-2} & , j=0 \\ n_\rho(n_\rho-1)(n_\rho-2)\tau(1-\tau)^{n_\rho-3}-2n_\rho(n_\rho-1)(1-\tau)^{n_\rho-2} & , j=1 \\ \dfrac{n_\rho!\tau^{j-2}(1-\tau)^{n_\rho-j}}{(j-2)!(n_\rho-j)!}-\dfrac{2n_\rho!\tau^{j-1}(1-\tau)^{n_\rho-j-1}}{(j-1)!(n_\rho-j-1)!}+\dfrac{n_\rho!\tau^{j}(1-\tau)^{n_\rho-j-2}}{j!(n_\rho-j-2)!} & , j\in[2,n_\rho-2] \\ n_\rho(n_\rho-1)(n_\rho-2)\tau^{n_\rho-3}(1-\tau)-2n_\rho(n_\rho-1)\tau^{n_\rho-2} & , j=n_\rho-1 \\ n_\rho(n_\rho-1)\tau^{n_\rho-2} & , j=n_\rho \end{cases} \end{cases} \tag{27}$$

The values of the Bezier basis functions and their derivatives at the boundary are:

$$\begin{cases} B_{\rho,j}(\tau=0)=\begin{cases} 1 & j=0 \\ 0 & j\in[1,n_\rho] \end{cases} \\ B'_{\rho,j}(\tau=0)=\begin{cases} -n_\rho & j=0 \\ n_\rho & j=1 \\ 0 & j\in[2,n_\rho] \end{cases} \end{cases} \quad \begin{cases} B_{\rho,j}(\tau=1)=\begin{cases} 0 & j\in[0,n_\rho-1] \\ 1 & j=n_\rho \end{cases} \\ B'_{\rho,j}(\tau=1)=\begin{cases} 0 & j\in[0,n_\rho-2] \\ -n_\rho & j=n_\rho-1 \\ n_\rho & j=n_\rho \end{cases} \end{cases} \tag{28}$$

Based on Eqs. (24) and (26), along with the boundary constraints, the following expression can be obtained:

$$\begin{cases} \rho_i=\rho(\tau=0)=P_{\rho,0} \\ T\dot{\rho}_i=\rho'(\tau=0)=n_\rho(P_{\rho,1}-P_{\rho,0}) \end{cases} \quad \begin{cases} \rho_f=\rho(\tau=1)=P_{\rho,n_\rho} \\ T\dot{\rho}_f=\rho'(\tau=1)=n_\rho(P_{\rho,n_\rho}-P_{\rho,n_\rho-1}) \end{cases} \tag{29}$$

The above expression can specifically determine the four Bezier coefficients $(P_{\rho,0},P_{\rho,1},P_{\rho,n_\rho-1},P_{\rho,n_\rho})$, which are expressed as follows:

$$\begin{cases} P_{\rho,0}=\rho_i \\ P_{\rho,n_\rho-1}=\rho_f-T\dot{\rho}_f/n_\rho \end{cases} \quad \begin{cases} P_{\rho,1}=\rho_i+T\dot{\rho}_i/n_\rho \\ P_{\rho,n_\rho}=\rho_f \end{cases} \tag{30}$$

The trajectory optimized using the Bezier basis function method needs to satisfy a series of constraint conditions. Therefore, discrete waypoints are defined along the transfer trajectory to apply path constraints on the magnetic sail propulsion system. To avoid the occurrence of the Runge phenomenon at the boundaries, the discrete points are chosen using Legendre-Gauss distribution, which corresponds to the roots of the *m*-th order Legendre polynomial. The discrete points are shown as follows:

$$\tau_0=0<\tau_1<\cdots<\tau_{m-1}=1 \tag{31}$$

For the dimensionless time τ, we consider these discrete points to be fixed throughout the entire optimization process. Therefore, τ can be represented as a column vector, and the three coordinate components along with their corresponding first and second derivatives with respect to τ can be expressed in the following matrix form:

$$\begin{cases}[\rho]_{m\times1}=[B_\rho]_{m\times(n_\rho+1)}[P_\rho]_{(n_\rho+1)\times1}\\ [\rho']_{m\times1}=[B'_\rho]_{m\times(n_\rho+1)}[P_\rho]_{(n_\rho+1)\times1}\\ [\rho'']_{m\times1}=[B''_\rho]_{m\times(n_\rho+1)}[P_\rho]_{(n_\rho+1)\times1}\end{cases} \tag{32}$$

where $[P_\rho]_{(n_\rho+1)\times1}$ are the Bezier coefficients, which can be expressed as follows:

$$[P_\rho]_{(n_\rho+1)\times1}=[P_{\rho,0}\quad P_{\rho,1}\quad [X_\rho]^{\mathrm{T}}_{(n_\rho-3)\times1}\quad P_{\rho,n_\rho-1}\quad P_{\rho,n_\rho}]^{\mathrm{T}} \tag{33}$$

where $[X_\rho]_{(n_\rho-3)\times1}$ are the unknown Bezier coefficients, expressed as follows:

$$[X_\rho]_{(n_\rho-3)\times1}=[P_{\rho,2},P_{\rho,3},\cdots,P_{\rho,n_\rho-3},P_{\rho,n_\rho-2}]^{\mathrm{T}} \tag{34}$$

The components of the thrust acceleration at each discrete point in the cylindrical coordinate system can also be expressed in matrix form as follows:

$$[a_\rho]_{m\times1}=a_\rho([\rho]_{m\times1},[z]_{m\times1},[\theta']_{m\times1},[\rho'']_{m\times1}) \tag{35}$$

When the order of the Bezier shape function and the discrete points are defined, the matrices for the Bezier basis functions and their derivatives are constant, irrespective of whether the total transfer time for the magnetic sail is known. This attribute ensures that the shape function matrices do not need to be recomputed in every iteration, thereby effectively minimizing computational load.

In the study of the single-target transfer problem, the total transfer time is a crucial indicator of performance. Therefore, we consider the total transfer time T as the optimization criterion.

Transform the thrust coefficient into matrix form $[\gamma]_{m\times1}$, and similarly convert the parameters D under the square root into matrix form $[D]_{m\times1}$. Thus, based on the above transformation relationships and the constraint condition given by Eq. (23), the optimization problem for the magnetic sail transfer trajectory is transformed into a nonlinear programming problem (NLP):

$$\begin{gathered}\min\ T\\ [X_\rho]_{(n_\rho-3)\times1},[X_\theta]_{(n_\theta-3)\times1},[X_z]_{(n_z-3)\times1},[T]\\ \text{s.t. } [\gamma]_{m\times1}\ge0,[\gamma]_{m\times1}\le1,[D]_{m\times1}\ge0,[a_{oz}]_{m\times1}\ge0\end{gathered} \tag{36}$$

3.2 Initial Value Guess

Using cubic Bezier shape functions ($n_\rho=n_\theta=n_z=3$) for the initial value estimation of the unknown Bezier coefficients:

$$\begin{aligned}\rho_{Inl}(\tau)&=(1-\tau)^3P_{\rho,0}+3\tau(1-\tau)^2P_{\rho,1}+3\tau^2(1-\tau)P_{\rho,2}+\tau^3P_{\rho,3}\\ \theta_{Inl}(\tau)&=(1-\tau)^3P_{\theta,0}+3\tau(1-\tau)^2P_{\theta,1}+3\tau^2(1-\tau)P_{\theta,2}+\tau^3P_{\theta,3}\\ z_{Inl}(\tau)&=(1-\tau)^3P_{z,0}+3\tau(1-\tau)^2P_{z,1}+3\tau^2(1-\tau)P_{z,2}+\tau^3P_{z,3}\end{aligned} \tag{37}$$

where the subscript '*Inl*' denotes the initial estimate of the corresponding variable. Based on Eq. (30), the values of the four Bezier coefficients under the three coordinate components are given by the following equation:

$$\begin{aligned}&\begin{cases}P_{\rho,0}=\rho_i\\ P_{\rho,2}=\rho_f-T_{Inl}\dot\rho_f/n_\rho\end{cases}\quad\begin{cases}P_{\rho,1}=\rho_i+T_{Inl}\dot\rho_i/n_\rho\\ P_{\rho,3}=\rho_f\end{cases}\\ &\begin{cases}P_{\theta,0}=\theta_i\\ P_{\theta,2}=\theta_f-T_{Inl}\dot\theta_f/n_\theta\end{cases}\quad\begin{cases}P_{\theta,1}=\theta_i+T_{Inl}\dot\theta_i/n_\theta\\ P_{\theta,3}=\theta_f\end{cases}\\ &\begin{cases}P_{z,0}=z_i\\ P_{z,2}=z_f-T_{Inl}\dot z_f/n_z\end{cases}\quad\begin{cases}P_{z,1}=z_i+T_{Inl}\dot z_i/n_z\\ P_{z,3}=z_f\end{cases}\end{aligned} \tag{38}$$

where T_{inl} represents the initial estimate for the magnetic sail transfer process. The discretized dimensionless time is as follows:

$$\tau_{Inl,0}=0<\tau_{Inl,1}<\cdots<\tau_{Inl,m}=1 \tag{39}$$

Therefore, substituting $\tau=\tau_{Inl}$ into Eq. (37) yields the matrix representation of the three coordinate components $[\rho_{Inl}],[\theta_{Inl}],[z_{Inl}]$. Since the basis of the Bezier shape functions is constant, we can further derive the initial estimate of the unknown Bezier coefficients as follows:

$$\begin{cases} [P_\rho]_{(n_\rho+1)\times 1,Inl} = \dfrac{[\rho_{Inl}]}{[B_\rho]_{m\times(n_\rho+1)}} \\ [P_\theta]_{(n_\theta+1)\times 1,Inl} = \dfrac{[\theta_{Inl}]}{[B_\theta]_{m\times(n_\theta+1)}} \\ [P_z]_{(n_z+1)\times 1,Inl} = \dfrac{[z_{Inl}]}{[B_z]_{m\times(n_z+1)}} \end{cases} \tag{40}$$

4. Simulation Verification Analysis

To evaluate the performance of the trajectory optimization technique grounded in Bezier shape functions, this study designs a classical Earth-Mars transfer scenario. The simulation parameters were set as follows: the Bezier curve's order and the count of Legendre-Gauss discretization points were established as $n_\rho = 12$, $n_\theta = 12$, $n_z = 10$ and $m = 40$. The optimization of the NLP problem was performed using the interior-point method, with the decision variable tolerance set to 10^{-8}, the objective function tolerance set to 10^{-8}, and the constraint tolerance set to 10^{-7}. Parallel computation was enabled.

Meanwhile, we will use the optimization results obtained from the Bezier method as the initial values for the Gaussian Pseudospectral Method (GPM) to further optimize the trajectory and compare the results. In the GPM, we set 80 discretization points and employed the Sequential Quadratic Programming (SQP) method to solve the NLP problem. All aforementioned procedures were executed utilizing the fmincon function. Simulations were take place on a personal computer platform equipped with an AMD 5800H CPU (base frequency 3.20 GHz) and 32 GB of RAM. The simulation results are as follows:

Set the parameters for the magnetic sail, $R = 40$ km and $f = 0.7$. Fig.5 shows the transfer trajectories of the magnetic sail spacecraft from Earth to Mars, optimized using the Bezier function method and the GPM. The blue curve represents the transfer trajectory optimized by the Bezier method, while the black curve indicates the result obtained by the GPM. The positions marked by pentagons represent the endpoints of the two transfer trajectories. Fig. 6 and 7 display the time-varying components of the position vector and velocity vector (in the spacecraft's orbital coordinate system) of the magnetic sail during the transfer process, respectively. It can be observed that both methods effectively meet the boundary conditions (launch and final position constraints and velocity constraints). Fig. 8 presents the variation of thrust coefficients during the transfer process for the two optimization methods. The blue curve represents the Bezier optimization method, while the black curve corresponds to the GPM. The red curve indicates the maximum thrust constraint. It can be observed that both methods are capable of satisfying the propulsion acceleration constraints. Fig. 9 illustrates the variation curves of each acceleration component during the transfer process, based on the Bezier function method. Fig. 10 illustrates the variation of the two attitude angles during the transfer process. It can be observed that both attitude parameters of the magnetic sail change continuously.

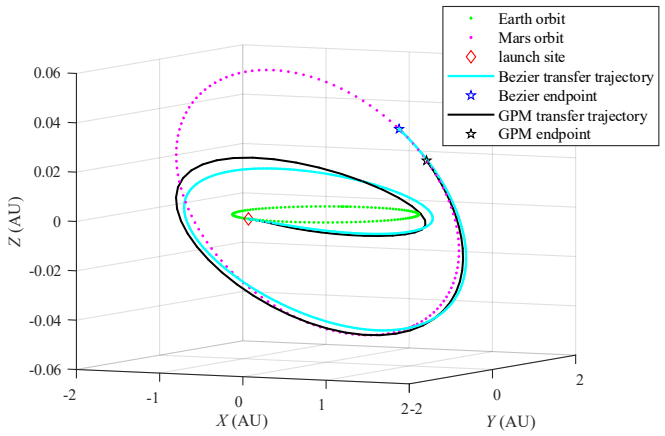

Fig.5 Magnetic Sail Earth-Mars Transfer Trajectory

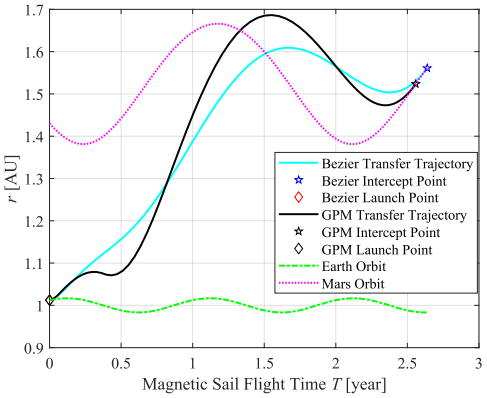

(a) Time-Varying Curve of Radial Position of the Magnetic Sail

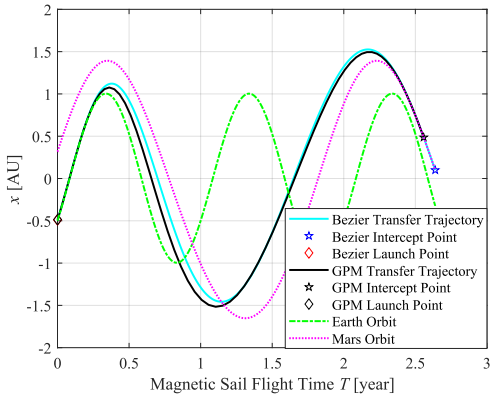

(b) Time-Varying Curve of the X-Axis Position of the Magnetic Sail

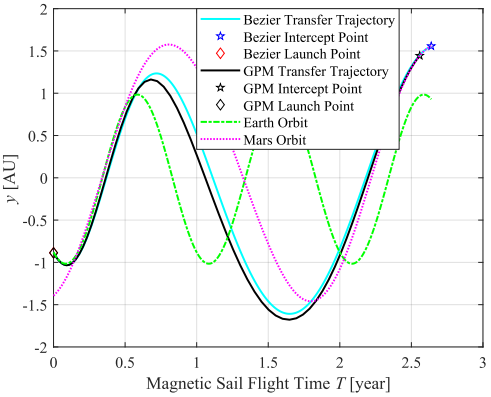

(c) Time-Varying Curve of the Y-Axis Position of the Magnetic Sail

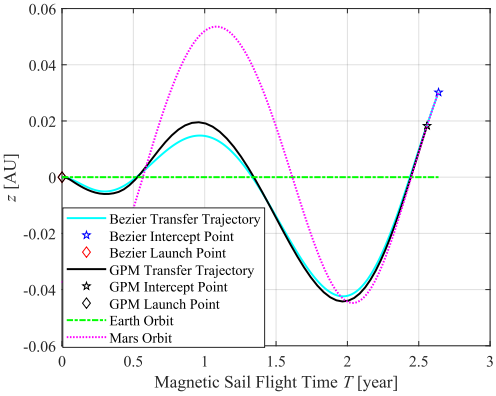

(d) Time-Varying Curve of the Z-Axis Position of the Magnetic Sail

Fig. 6 Time-Varying Curves of the Position Vector Components of the Magnetic Sail During the Transfer Process

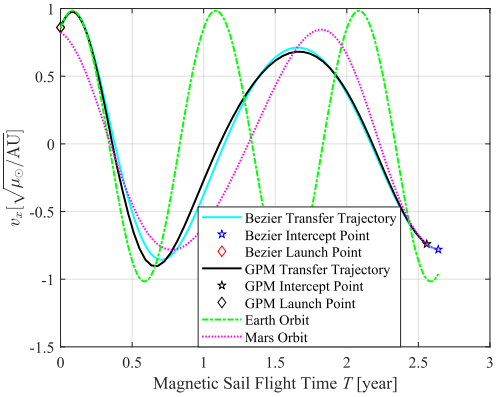

(a) Time-Varying Curve of the X-Axis Velocity of the Magnetic Sail

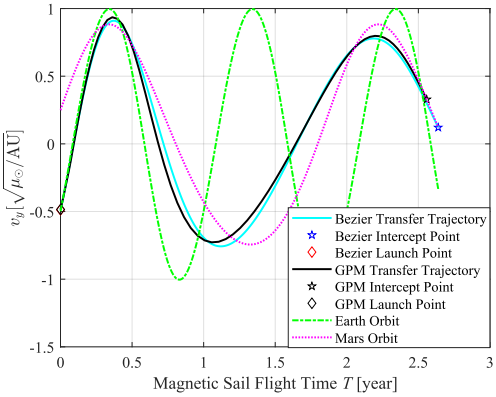

(b) Time-Varying Curve of the Y-Axis Velocity of the Magnetic Sail

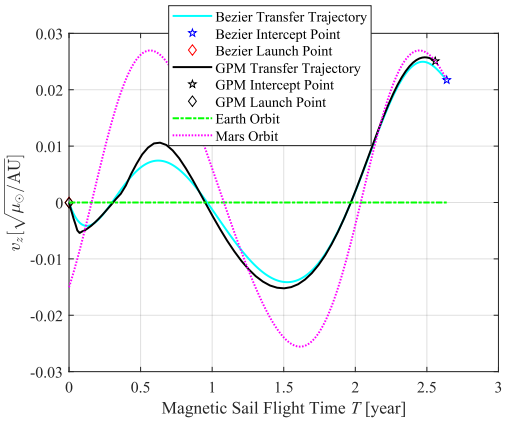

(c) Time-Varying Curve of the Z-Axis Velocity of the Magnetic Sail

Fig.7 Time-Varying Curves of the Velocity Vector Components of the Magnetic Sail

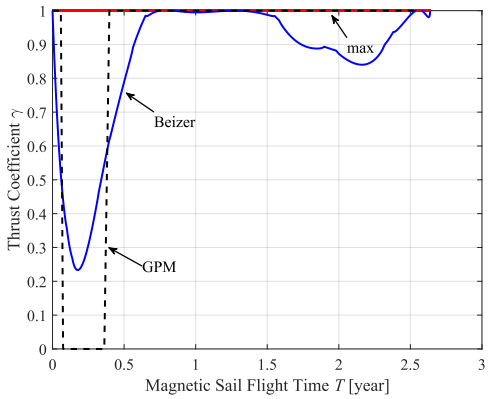

Fig.8 Variation Curve of the Propulsion Coefficient Required for the Transfer Trajectory of the Magnetic Sail

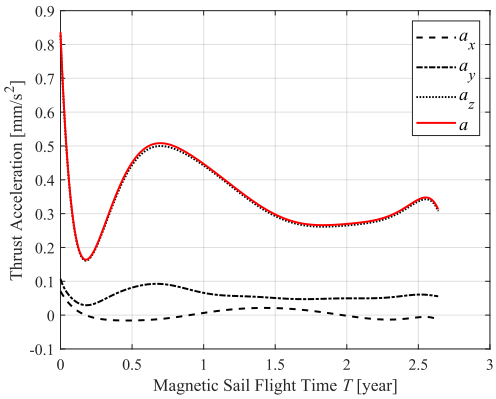

Fig.9 Variation Curve of the Propulsive Acceleration Components During Transfer Obtained Using the Bezier Function Method

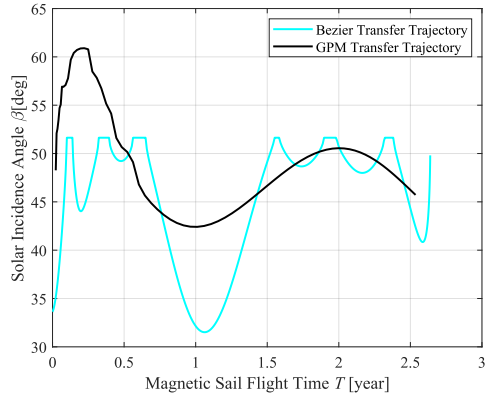

(a) Variation Curve of the Solar Incidence Angle Over Time During the Magnetic Sail Transfer Process

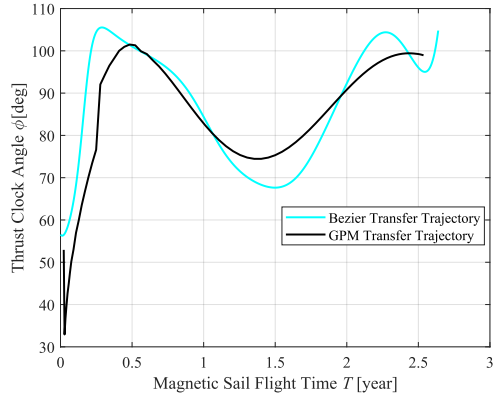

(b) Variation Curve of the Propulsion Cone Angle Over Time During the Magnetic Sail Transfer Process

Fig.10 Variation of the Two Attitude Angles During the Transfer Process

This study adjusted the coil radius of the magnetic sail to modify the maximum propulsive acceleration, and compared the transfer processes of the magnetic sail spacecraft under different maximum propulsive accelerations, the results are shown in Fig.11. The results indicate that when the magnetic sail coil radius R is less than 50 km, the total transfer time decreases rapidly as the R increases, whereas for R greater than 50 km, the decrease in total transfer time

is more gradual. Fig.12 shows the variation curves of the propulsion coefficient during the transfer process for magnetic sail coil radius of R = 30 km and R = 100 km, respectively. When R<50 km, the propulsion coefficient γ remains equal to 1 for most of the duration, with the maximum thrust constraint exerting a significant influence, thereby causing the total transfer time to vary dramatically with changes in the magnetic sail coil radius. In contrast, for R>50 km, the optimal transfer trajectory is characterized by an extended gliding phase, with the maximum thrust constraint having a relatively minor effect, thereby resulting in comparatively gradual variations in the total transfer time.

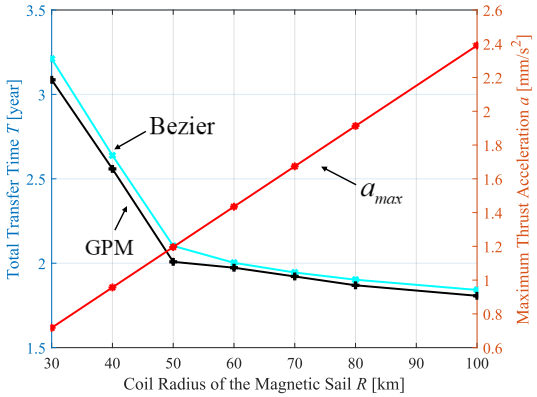

Fig.11 Variation Curves of Transfer Time and Maximum Thrust Acceleration of the Magnetic Sail with Respect to Coil Radius

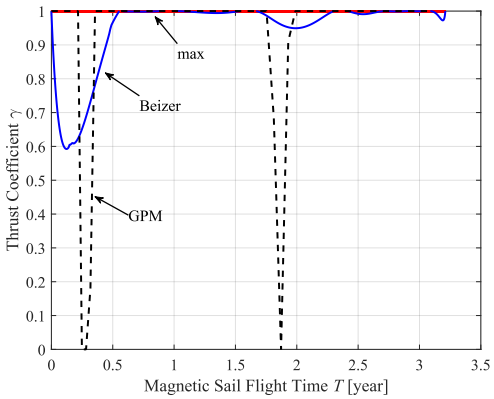

(a) R=30km Thrust Coefficient Variation Curve

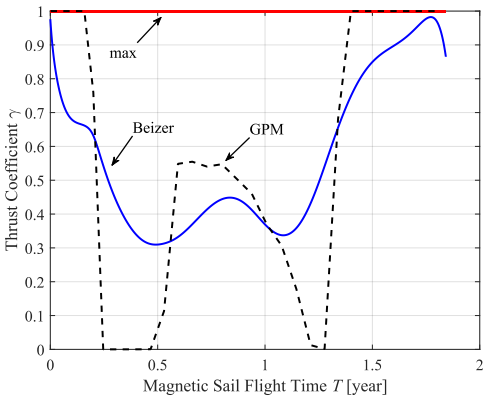

(b) R=100km Thrust Coefficient Variation Curve

Fig.12 Variation Curves of the Propulsion Coefficient during the Magnetic Sail Transfer Process for Different Coil Radius

Table 2 Simulation Results of the Earth-Mars Transfer Process

R [km]	a_c [mm / s^2]	Total Transfer Time T [year]		Simulation Computation Time t_{cpu} [s]	
		Bezier	GPM	Bezier	GPM
30	0.718	3.210	3.093	82.167	2033.484
40	0.957	2.638	2.560	79.324	1784.064
50	1.196	2.102	2.083	68.194	1474.268
60	1.435	2.001	1.975	75.892	1653.271
70	1.674	1.945	1.923	72.472	1723.595
80	1.913	1.902	1.871	77.031	1680.755
100	2.390	1.841	1.810	75.382	1769.582

The performance metrics and computation times of the two optimization methods are presented in Table 2. The average total flight time for the magnetic sail Earth-Mars transfer trajectory differs by only 1.839% between the two methods. The average computation time for optimizing the magnetic sail trajectory using the Bezier function method is only 4.393% of that required by the GPM.

To validate the universality of the Bessel method, this study also designed a mission scenario for the magnetic sail's escape from the solar system. In this three-dimensional trajectory design, the order of the Bezier shape function is set to $n_\rho = 6$, $n_\theta = 6$, $n_z = 6$, with a total of $m = 120$ discrete points. The remaining parameters are consistent with those of the magnetic sail transfer mission to Mars. Similarly, after designing the trajectory using the Bezier method,

we further optimized the trajectory using the GPM.

Fig.13 presents the results of the optimized transfer trajectory for the magnetic sail escaping the solar system, obtained using the Bezier method and the GPM. The results above indicate that the transfer trajectories obtained by the two methods are quite similar, with the final coordinates being almost identical. Fig.14 illustrates the variation of thrust coefficients over time corresponding to the transfer trajectories obtained by the two methods, showing that both methods satisfy the acceleration constraints of the magnetic sail. Fig.15 presents the time-dependent components of thrust acceleration obtained using the Bezier method.

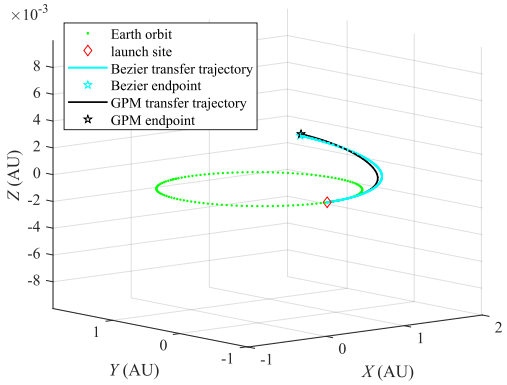

Fig.13 Magnetic Sail Escaping Solar System Transfer Trajectory

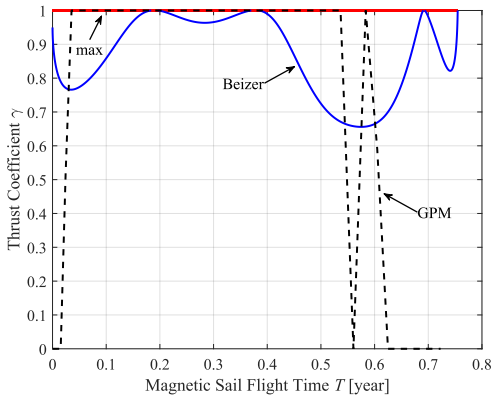

Fig.14 Variation Curve of the Propulsion Coefficient Required for the Transfer Trajectory of the Magnetic Sail

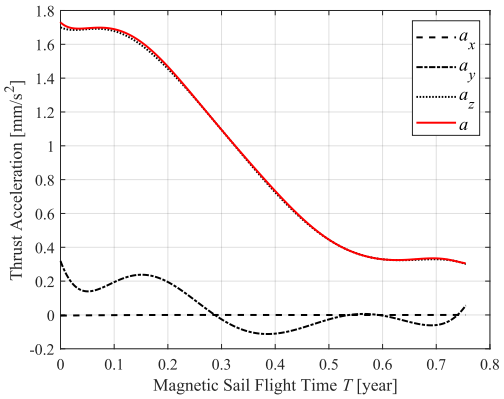

Fig.15 Variation Curve of the Propulsive Accelera-tion Components During Transfer Obtained Using the Bezier Function Method

The performance metrics and computation times of the two methods under the aforementioned task scenario are presented in Table 3. The transfer time results obtained from both methods differ by only 3.98%, while the computational speed using the Bezier method is approximately 100 times faster than that of the GPM.

Table 3 Simulation Results of Escaping the Solar System

Method	Total Transfer Time T [year]	Simulation Computation Time t_{cpu} [s]
Bezier	0.754	18.823
GPM	0.724	1832.331

From the above two simulation scenarios, it can be concluded that the Bezier method demonstrates good performance in the rapid computation of transfer trajectories for the magnetic sail, making it highly suitable for solving a large number of simulation cases during the initial task design phase. Additionally, the magnetic sail thrust acceleration model proposed in this study can effectively facilitate the performance design of the magnetic sail in the early stages of the mission.

5. Conclusions

This study proposes a rapid trajectory optimization method for magnetic sails based on Bezier functions. By rigorously controlling the current in the magnetic sail coils, an improved model for magnetic sail propulsion acceleration is obtained, which is better suited for interplanetary missions. The study investigates boundary constraints during

the transfer process and constraints related to the thrust characteristics of the magnetic sail. Utilizing the state variables represented by Bezier functions for estimation, the trajectory optimization problem is transformed into a NLP problem according to the constraints. To validate the utility of the introduced method, we set up a transfer scenario between Earth and Mars and optimized the three-dimensional transfer trajectory of the magnetic sail. Results from the simulation demonstrate that the Bezier approach can rapidly create transfer trajectories that conform to the given constraints, with performance differing by less than 2% compared to the GPM, and a computational efficiency improvement of approximately 23 times, significantly saving time and resources. Additionally, this approach provides an efficient tool for magnetic sail system design, revealing the nonlinear relationship between coil radius and minimum flight time, thus offering a theoretical foundation for the planning of deep space exploration missions. At the same time, in order to validate the universality of the proposed method, a task scenario for the magnetic sail's escape from the solar system was established. The results indicate that the Bezier method not only maintains trajectory optimization accuracy (with a discrepancy of 3.98% compared to the GPM) but also demonstrates excellent computational efficiency (improving by 100 times compared to GPM). This proves vital for swiftly analyzing various magnetic sail mission setups in early design stages.

References

[1] Berthet M, Schalkwyk J, çelik O, et al. Space sails for achieving major space exploration goals: Historical review and future outlook[J]. Progress in Aerospace Sciences. 2024, 150: 101047.
[2] Fu B, Sperber E, Eke F. Solar sail technology—A state of the art review[J]. Progress in Aerospace Sciences. 2016, 86: 1-19.
[3] A. A Q, G. M, L. N, et al. Solar Sail Augmented Hohmann Transfer[J]. IEEE Transactions on Aerospace and Electronic Systems. 2023, 59(2): 2065-2071.
[4] Zhao P, Wu C, Li Y. Design and application of solar sailing: A review on key technologies[J]. Chinese Journal of Aeronautics. 2023, 36(5): 125-144.
[5] Bassetto M, Quarta A A, Mengali G, et al. Trajectory Analysis of a Sun-Facing Solar Sail with Optical Degradation[J]. Journal of Guidance, Control, and Dynamics. 2020, 43(9): 1727-1732.
[6] Bassetto M, Niccolai L, Quarta A A, et al. A comprehensive review of Electric Solar Wind Sail concept and its applications[J]. Progress in Aerospace Sciences. 2022, 128: 100768.
[7] Lingam M, Loeb A. Electric sails are potentially more effective than light sails near most stars[J]. Acta Astronautica. 2020, 168: 146-154.
[8] Bassetto M, Quarta A A, Mengali G. Thrust model and guidance scheme for single-tether E-sail with constant attitude[J]. Aerospace Science and Technology. 2023, 142: 108618.
[9] Zubrin R M, Andrews D G. Magnetic sails and interplanetary travel[J]. Journal of Spacecraft and Rockets. 1991, 28(2): 197-203.
[10] Quarta A A, Mengali G, Aliasi G. Optimal control laws for heliocentric transfers with a magnetic sail[J]. Acta Astronautica. 2013, 89: 216-225.
[11] Bassetto M, Quarta A A, Mengali G. Magnetic sail-based displaced non-Keplerian orbits[J]. Aerospace Science and Technology. 2019, 92: 363-372.
[12] Bassetto M, Perakis N, Quarta A A, et al. Refined MagSail thrust model for preliminary mission design and trajectory optimization[J]. Aerospace Science and Technology. 2023, 133: 108113.
[13] Petropoulos A E, Longuski J M. Shape-Based Algorithm for the Automated Design of Low-Thrust, Gravity Assist Trajectories[J]. Journal of Spacecraft and Rockets. 2004, 41(5): 787-796.
[14] Wall B J, Conway B A. Shape-Based Approach to Low-Thrust Rendezvous Trajectory Design[J]. Journal of Guidance, Control, and Dynamics. 2009, 32(1): 95-101.
[15] Xie C, Zhang G, Zhang Y. Simple Shaping Approximation for Low-Thrust Trajectories Between Coplanar Elliptical Orbits[J]. Journal of Guidance, Control, and Dynamics. 2015, 38(12): 2448-2455.
[16] Peloni A, Dachwald B, Ceriotti M. Multiple near-earth asteroid rendezvous mission: Solar-sailing options[J]. Advances in Space Research. 2018, 62(8): 2084-2098.
[17] Abdelkhalik O, Taheri E. Approximate On-Off Low-Thrust Space Trajectories Using Fourier Series[J]. Journal of Spacecraft and Rockets. 2012, 49(5): 962-965.
[18] Huo M, Mengali G, Quarta A A, et al. Electric sail trajectory design with Bezier curve-based shaping approach[J]. Aerospace Science and Technology. 2019, 88: 126-135.
[19] Zubrin R M. The use of magnetic sails to escape from low earth orbit[M]. American Institute of Aeronautics and Astronautics, 1991.
[20] Zhao L, Yuan C, Gong S, et al. Formation flying for magnetic sails around artificial equilibrium points[J]. Advances in Space Research. 2023, 71(3): 1605-1626.

Chinese Journal of Aeronautics

投 稿 表

题目	Optimizing Interplanetary Trajectories Bezier Shape-Based Method Applied to Magnetic Sail			
全部作者	姓名	职务(职称)	单位	E-mail
	姚博锐		哈尔滨工业大学	ybr_hit@163.com
	金如浩		哈尔滨工业大学	22B918084@stu.hit.edu.cn
	赵汗青		哈尔滨工业大学	zhaohanqing2002@163.com
	郝梓淇		哈尔滨工业大学	hzq18811469047@163.com
	王乐涵		哈尔滨工业大学	210079405@qq.com
	姜钧昊		哈尔滨工业大学	24S018077@stu.hit.edu.cn
	石雨豪		哈尔滨工业大学	24B918061@hit.edu.cn
	付翌航		哈尔滨工业大学	1561145149@qq.com
	岳佳琦		哈尔滨工业大学	2382068053@qq.com
	霍明英	教授	哈尔滨工业大学	huomingying@hit.edu.cn
备注：投稿表中必须按顺序写出作者姓名和单位（有两个单位的均要写出），最后录用出版的作者信息以此为准，作者的姓名、数量和责任单位均不得更改。				
联系人	姓名: 霍明英 座机:			
	手机: 15045129385 E-mail: huomingying@hit.edu.cn			
	通信(邮编、地址): 150001 哈尔滨市南岗区西大直街 92 号哈工大一校区新技术楼 408			
课题背景	This work was supported by the National Natural Science Foundation of China (grant no. U22B2013), Shanghai Aerospace Science and Technology Innovation Fund (grant no. SAST2023-089), and Natural Science Foundation of Heilongjiang Province (grant no. YQ2023A003).			
推荐审稿人 (可选)	姓名	职务(职称)	通信(邮编)	
回避审稿人 (可选)	姓名	职务(职称)	通信(邮编)	
附言 (可选)	如：因某种理由急于发表；或限投中文版(或英文版)学报；或只接受作为综述(或论文，研究简报)录用的；或联系地址将变更的等。退稿后经过改进再投稿的请说明原文章编号。			

保 密 审 查 证 明

《Chinese Journal of Aeronautics》编辑部：

经审查，我单位姚博锐等同志的投往贵刊的文章“Optimizing Interplanetary Trajectories Bezier Shape-Based Method Applied to Magnetic Sail”内容（**包括但不限于论文题目、作者署名及单位、基金项目、文字内容、图片、数据**）不涉及国家秘密、工作秘密和敏感信息，可以公开发表。

特此证明。

保密部门盖章：

2019年6月10日

本单位确无保密部门，本文作者承诺本论文内容（**包括但不限于论文题目、作者署名及单位、基金项目、文字内容、图片、数据**）不涉及国家秘密、工作秘密和敏感信息，可公开发表。

负责人签名：_____

单位公章：

年　月　日

版 权 转 让 协 议 及 投 稿 承 诺

论文题目： Optimizing Interplanetary Trajectories Bezier Shape-Based Method Applied to Magnetic Sail

文章摘要： Interplanetary spaceflight is one of the indispensable means for deep space exploration, yet it is highly constrained by the limitations imposed by fuel loading. As a propulsion system that operates without fuel, magnetic sails have garnered increasing attention and research focus due to their high thrust-to-weight ratio. This study adopts the latest Single-Loop Magnetic Sail(SiLM) thrust model and employs precise control of the coil current to construct an improved magnetic sail thrust model, thereby enhancing its suitability for complex deep-space exploration missions. To achieve rapid trajectory optimization for magnetic sail interplanetary missions, this study proposes an optimization strategy based on Bezier curve parameterization. Assuming that the variation of the magnetic sail state parameters follows a Bezier curve form, the Bezier coefficients are op-timized under a time-optimal objective to satisfy the equations of motion and constraint conditions. In this study, a typical deep space exploration scenario is designed for simulation validation. The results obtained using the Bezier method serve as the initial guess for the Gauss Pseudospectral Method(GPM), which is subsequently further optimized to compare the performance of the two methods. In the Earth-to-Mars transfer mission val-idation, the trajectory accuracy difference between the Bezier method and the GPM was less than 2%, while the computational speed of Bezier method increased by approximately 23 times, underscoring its advantages in rapid analysis for multiple scenarios during the early mission phases. Furthermore, the influence of magnetic sail design parameters on the transfer trajectory was investigated. By altering the magnetic sail coil radius, a nonlinear relationship curve between the shortest flight time and the coil radius was obtained, providing sig-nificant guidance for the design of magnetic sail performance parameters. In the validation of the solar system escape mission, the Bezier method still maintained excellent performance advantages, demonstrating its uni-versality. This study developed an improved magnetic sail thrust model and a rapid trajectory optimization method, providing an efficient theoretical tool for orbit design and system parameter optimization in deep space exploration missions.

全体作者： 姚博锐、金如浩、赵汗青、郝梓淇、王乐涵、姜钧昊、石雨豪、付翌航、岳佳琦、霍明英*

遵照《中华人民共和国著作权法》，自本协议签署之日起，上述论文全体作者同意：一经录用，全体作者将上述论文（各种语言版本）所享有的复制权、发行权、信息网络传播权、改编权、翻译权、汇编权，在作品的有效期内及在全世界范围内**转让**给航空学报杂志社，航空学报杂志社许可第三方出版或在线上传播论文时不再需要全体作者同意。就此转让事宜，全体作者**同意**不收取转让费用。全体作者许可航空学报杂志社根据实际需要代理申请上述作品的各种语言版本（包含各种介质）的版权登记事宜。

（1）在声明航空学报杂志社拥有该文版权的情况下，全体作者可以自由行使下列各项权利：

① 该文在《Chinese Journal of Aeronautics》上发表后，作者可以许可第三方在不使用《Chinese Journal of Aeronautics》版式设计且不是用于在其他刊物发表的前提下，重新出版该文或其译文或摘录。如使用上述刊物版式(含各种介质、媒体版式，下同)，则必须获得上述刊物编辑部的书面许可。

② 该文在《Chinese Journal of Aeronautics》上发表后，作者有权在汇编个人文集或以其他方式(含作者个人

网页中)出版个人作品时，不经修订地全部或部分使用该文上述版式。

③ 作者有权将该文上传到网络服务器上并更新该文，但为此目的不得使用《Chinese Journal of Aeronautics》或其经销商制作的数字化和/或版式化的文档。该文发表后，作者实施本项行为时应附有与上述刊物的在线文摘或该刊物的进入主页的链接。

④ 如果该文作者是为完成法人或其他组织的工作任务所创作的作品属于职务作品范围，法人或其他组织有权在其业务范围内复制该文用于其个人内部使用。

（2）全体作者对投稿论文作出以下承诺：

① 稿件为全体作者的原创研究成果，不存在任何侵权行为，包括但不限于不侵犯任何第三方的著作权及其它知识产权、肖像权、名誉权，也不存在《学术出版规范——期刊学术不端行为界定（CY/T174—2019）》中的各项学术不端行为。

② 稿件全部或实质性部分未曾发表过，也未将其投往其他期刊、杂志，亦没有在先将有关著作权许可给任何第三方。

③ 稿件作者署名及署名顺序、基金资助等信息已经经过全部作者的审核和同意，投稿后不再修改；稿件内容自编辑审稿定稿后不再修改；如因上述修改给航空学报杂志社造成损失的，由全体作者连带赔偿。

④ 同意《Chinese Journal of Aeronautics》的审稿费用、出版费用。因本刊稿酬已抵消部分版面费，故不再额外支付稿酬。

⑤ 若从 *Chinese Journal of Aeronautics* 编辑部收到本稿起 3 个月内作者未收到本文的修改、录用或退稿通知，作者有权改投他刊，但保证事先通知本刊。

⑥ 保密承诺：本次及后续提交的各版次稿件的各项要素（包括但不限于论文题目、作者署名及单位、基金项目、文字内容、图片、数据）均不涉及国家秘密、工作秘密和敏感信息，可以公开发表及在互联网传播。

注意：本刊要求发表的论文具有首发权，因此如果论文主要内容已在会议文集或是在预印本网站公开发表，本刊不接受投稿。

请第一作者在右侧手写："已充分理解并同意上述条款"： 已充分理解并同意上述条款

请全体作者签名表示理解并同意上述条款（不得代签，如有特殊情况可与编辑部联系）、日期：

导师签字（研究生投稿）、日期： 霍旭昊
2025年6月4日

姚博锐
金加喆
石雨豪
赵祥清
郝祥淇
王乐涵
岳佳琦
付翌航
善钢昊

2025年6月4日

Declaration of Interest Statement

☐ The authors declare that they have no known competing financial interests or personal relationships that could have appeared to influence the work reported in this paper.

☐ The author is an Editorial Board Member/Editor-in-Chief/Associate Editor/Guest Editor for this journal and was not involved in the editorial review or the decision to publish this article.

☒ The authors declare the following financial interests/personal relationships which may be considered as potential competing interests:

Mingying Huo reports financial support was provided by National Natural Science Foundation of China. Mingying Huo reports financial support was provided by Shanghai Aerospace Science and Technology Innovation Fund. Mingying Huo reports financial support was provided by Natural Science Foundation of Heilongjiang Province. If there are other authors, they declare that they have no known competing financial interests or personal relationships that could have appeared to influence the work reported in this paper.